

## Interactions of 3.7-GeV/c Antiprotons with Ag and Br†

SEYMOUR KATCOFF

Chemistry Department, Brookhaven National Laboratory, Upton, New York

(Received 1 December 1966)

Stars produced in low-sensitivity nuclear emulsions by 3.7-GeV/c antiprotons are compared with stars produced by protons of about the same momentum. The reaction cross section of the antiprotons is 880 mb for production of stars which can be identified as originating in Ag or Br (410 mb for protons). The  $\alpha$ -particle and light-fragment prong distributions show that the antiprotons produce larger stars and therefore deposit more energy in the target nuclei. The production cross section for  $\alpha$ 's is 2750 mb; for light fragments ( $3 \leq Z \leq 6$ ), 710 mb; for  $\text{Li}^8$  fragments,  $\sim 29$  mb. For proton-induced stars, these cross sections are 960, 270, and  $\sim 4$  mb, respectively. The angular distribution of the recoiling residual nuclei is considerably less forward-peaked for antiproton irradiation.  $\alpha$ -particle spectra show that antiprotons yield a broader distribution and relatively more low-energy particles. The angular distributions of both  $\alpha$ 's and light fragments are, respectively, very similar for the two types of irradiation.

## I. INTRODUCTION

THE effects on complex nuclei of interactions with antiprotons have been studied only to a very limited extent. Very recently a paper by Bell *et al.*<sup>1</sup> has appeared on the nuclear interactions of 2-GeV antiprotons and negative pions with aluminum and carbon. Cross-section ratios for production of  $\text{C}^{11}$  from C and Al, and of  $\text{F}^{18}$  from Al were compared for the two different incident particles. The authors concluded that no significant differences were found within the experimental uncertainty of about 25%. Poskanzer and Remsberg<sup>2</sup> reported, in a reference, a preliminary measurement of the  $\text{C}^{12}(\bar{p}, \bar{p}n)\text{C}^{11}$  cross section for 2.8-GeV antiprotons. The value is  $30 \pm 9$  mb and it may be compared with 27.1 mb for production of  $\text{C}^{11}$  by incident protons of the same kinetic energy.

Although these fragmentary results do not show any substantial differences between the effects of interaction with antiprotons and protons, or pions, certain differences are to be expected because of the antiproton-nucleon annihilation process. In fact, it is instructive to compare (Table I) several  $\bar{p}p$  cross sections with the corresponding  $pp$  cross sections.<sup>3-8</sup> The antiproton annihilation cross section is included in  $\sigma_{\text{inel}}$ . At 2.5-GeV, it is 34 mb while the inelastic cross section *without annihilation* is 19 mb. Interactions with neutrons have

approximately the same cross sections as interactions with protons at incident energies above 400 MeV. It is seen that at relatively low energies (in the few hundred MeV region) the total cross section for  $\bar{p}p$  is about six times as large as for the  $pp$  interaction, while the elastic cross section is about twice as large. At higher energies, these differences diminish, but at 2.5 GeV the  $\bar{p}p$  elastic cross section is still 60% larger and  $\sigma_{\text{inel}}$  is 80% larger than the corresponding  $pp$  cross sections.

During annihilation, an average of five or more pions are produced.<sup>9</sup> When this occurs in a complex nucleus some of these pions may be reabsorbed with the deposition of a large amount of energy. Thus one might find that antiprotons are more likely than protons to induced nuclear reactions which require higher excitation energies. Perhaps fragmentation would be more prevalent, and perhaps the production of lower-mass residual nuclei would be more probable. To test these ideas, low sensitivity nuclear emulsions were irradiated by 2.9-GeV antiprotons. The stars produced in the Ag and Br were analyzed in the same way as was done earlier<sup>10-12</sup> when the incident particles were protons.

TABLE I. Comparison of antiproton-nucleon and proton-nucleon total, elastic, and inelastic cross sections (mb).

$E(\text{lab})$ (GeV)	$\sigma_t$	$\bar{p}p$ $\sigma_{\text{el}}$	$\sigma_{\text{inel}}^a$	$\sigma_t$	$pp$ $\sigma_{\text{el}}$	$\sigma_{\text{inel}}$
0.1	180	64	116	26	26	
0.4	120	44	76	26	24	2
0.6	115	40	75	36	25	12
1.0	96	30	66	48	21	27
2.0	78	24	54	45	16	28
2.5	75	22	53	43	14	29
5.0	59			41	10	30
20.0	48			39	8	30

<sup>a</sup> Annihilation cross section included; at 2.5 GeV, this amounts to 34 mb.

† Research performed under the auspices of the U. S. Atomic Energy Commission.

<sup>1</sup> W. C. Bell, R. Brandt, K. F. Chackett, W. W. Neale, and H. L. Ravn, *Z. Naturforsch.* **21a**, 1042 (1966).

<sup>2</sup> A. M. Poskanzer and L. P. Remsberg, *Phys. Rev.* **134**, B779 (1964), Ref. 12 therein.

<sup>3</sup> W. Galbraith, E. W. Jenkins, T. F. Kycia, B. A. Leontic, R. H. Phillips, A. L. Read, and R. Rubinstein, *Phys. Rev.* **138**, B913 (1965).

<sup>4</sup> U. Amaldi, Jr., T. Fazzini, G. Fidecaro, C. Ghesquière, M. Legros, and H. Steiner, *Nuovo Cimento* **34**, 825 (1964).

<sup>5</sup> T. Ferbel, A. Firestone, J. Sandweiss, H. D. Taft, M. Gailloud, T. W. Morris, A. H. Bachman, P. Baumel, and R. M. Lea, *Phys. Rev.* **137**, B1250 (1965).

<sup>6</sup> T. Elioff, L. Agnew, O. Chamberlain, H. Steiner, C. Wiegand, and T. Ypsilantis, *Phys. Rev.* **128**, 869 (1962).

<sup>7</sup> D. V. Bugg, D. C. Salter, G. H. Stafford, R. F. George, K. F. Riley, and R. J. Tapper, *Phys. Rev.* **146**, 980 (1966).

<sup>8</sup> V. S. Barashenkov and V. M. Maltsev, *Fortschr. Physik* **9**, 549 (1961).

<sup>9</sup> T. Ferbel, A. Firestone, J. Sandweiss, H. D. Taft, M. Gailloud, T. W. Morris, W. J. Willis, A. H. Bachman, P. Baumel, and R. M. Lea, *Phys. Rev.* **143**, 1096 (1966).

<sup>10</sup> E. W. Baker, S. Katcoff, and C. P. Baker, *Phys. Rev.* **117**, 1352 (1960).

<sup>11</sup> E. W. Baker and S. Katcoff, *Phys. Rev.* **123**, 641 (1961).

<sup>12</sup> E. W. Baker and S. Katcoff, *Phys. Rev.* **126**, 729 (1962).

TABLE II. Summary of cross-section data: stars produced by 2.9-GeV antiprotons and by 3.0-GeV protons. Statistical uncertainties can be estimated from the observed numbers of stars and tracks.

Type of star	2.9-GeV antiprotons				3.0-GeV protons			
	I	II	III	Total	I	II	III	Total
Stars observed, number	347	259	27	633	272	177	65	514
Fraction of total stars	0.55	0.41	0.04	1.00	0.53	0.34	0.13	1.00
Stars, cross section (mb)	480	360	40	880	220	140	50	410
$\alpha$ particles, corr. number <sup>a</sup>	1093	851	43	1987	647	407	155	1209
$\alpha$ 's per star	3.15	3.29	1.6	3.14	2.38	2.30	2.39	2.35
$\alpha$ 's, cross section (mb)	1510	1180	60	2750	520	320	120	960
Light fragments, corr. number <sup>a</sup>	...	505	~6	511	...	295	41	336
Fragments per star	...	1.95	~0.2	0.81	...	1.67	0.63	0.65
Fragments, cross section (mb)	...	700	~10	710	...	240	30	270
Fragments per $\alpha$	...	0.59	~0.14	0.26	...	0.72	0.26	0.28
Li <sup>8</sup> , observed number	...	15	...	15	...	13 <sup>b</sup>	...	13 <sup>b</sup>
Li <sup>8</sup> , corrected number <sup>a</sup>	...	21	...	21	...	4.3 <sup>b</sup>	...	4.3 <sup>b</sup>
Li <sup>8</sup> , cross section (mb)	...	~29	...	~29	...	~4	...	~4

<sup>a</sup> Corrected for particles leaving the emulsion.

<sup>b</sup> A total of 2158 proton-induced stars were scanned for hammer tracks; the corrected number is normalized to 514 stars.

As will be discussed below, evidence was found that antiprotons do lead to higher excitation energies in the struck nuclei.

## II. EXPERIMENTAL

The separated 3.66-GeV/c antiproton beam which was used at the Brookhaven AGS has been described previously.<sup>5</sup> The purity of this beam<sup>13</sup> was about 95%. In the vertical plane it was 0.3-cm high and in the horizontal plane 5.0-cm wide (total width at half-intensity). Ilford K.0 and K.-1 nuclear emulsions, 200- $\mu$  thick, were irradiated for 3.9 h with the antiprotons entering at 20° to the surface. Each of these plates was covered with an Ilford G.5 pellicle, 100- $\mu$  thick, in order to monitor the incident antiproton beam. In addition, another G.5 pellicle was exposed perpendicular to the beam for more accurate monitoring and for measurement of the intensity distribution. A minimum of wrapping and supporting structure was used for the plates in order to minimize effects due to secondary particles.

The plates were processed in such a manner that both K.0 and K.-1 emulsions had the same effective sensitivity. Protons did not register tracks; only  $\alpha$  particles and heavier fragments were recorded. The stars which resulted from interactions with Ag and Br nuclei were identified by the same criteria that were used in earlier work.<sup>10,11</sup> A total of 3.60 cm<sup>2</sup> was area-scanned twice, and 633 acceptable stars were found. The scanning efficiency was 95%. The stars were classified into three types: group I, in which only  $\alpha$  particles and a recoil were observed; group II, in which light fragments ( $3 \leq Z \leq 6$ ) were observed in addition to the  $\alpha$ 's and re-

coil; and group III, in which two short, very heavily ionizing tracks are seen rather than one recoil.<sup>14</sup>

The G.5 pellicles were carefully scanned for beam tracks over the area which was used in the insensitive emulsions. The method of scanning was similar to that used previously for C<sup>12</sup>(*p, pn*)C<sup>11</sup> cross-section measurements.<sup>15</sup> About 5 000 tracks were counted in the pellicle

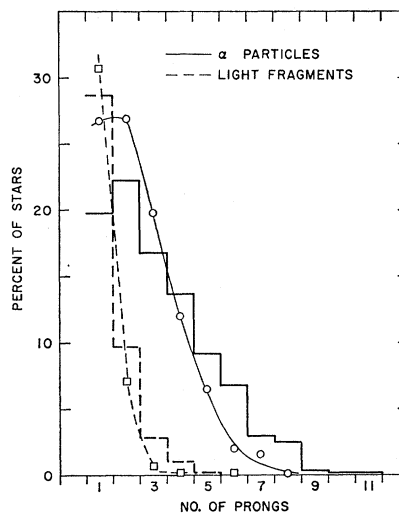


FIG. 1. Prong distributions of  $\alpha$  particles and light fragments. The histograms are for antiproton irradiation, the smooth curves and the points are for proton irradiation.

<sup>14</sup> In previous papers (Refs. 10-12), type-III events were called "fission." It was estimated that the most probable mass for these "fission fragments" is in the neighborhood of 35 amu. P. A. Gorichev, O. V. Lozhkin, and N. A. Perfilov {Zh. Eksperim. i Teor. Fiz. 45, 1784 (1963) [English transl.: Soviet Phys.—JETP 18, 1222 (1964)]} have estimated that one of the two fragments in this type of event is of somewhat lighter mass while the other one is the residual recoil nucleus. Therefore, they classify these events as fragmentation.

<sup>15</sup> J. B. Cumming, G. Friedlander, and S. Katcoff, Phys. Rev. 125, 2078 (1962).

<sup>13</sup> The beam layout is shown in Fig. 1 of Ref. 5. This experiment was located in front of slit No. 4. The possibility of neutron contamination is ruled out by the fact that the star density in the emulsion follows the same narrow distribution as the beam tracks recorded in the G.5 pellicle.

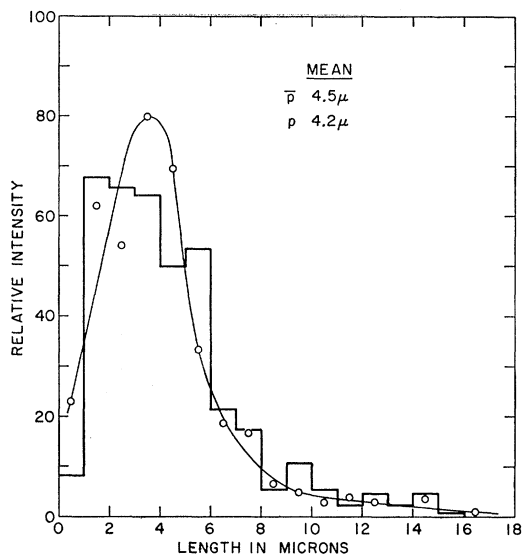


Fig. 2. Distribution of recoil ranges of residual nuclei. Histogram—antiproton irradiation; curve with points—proton irradiation.

exposed perpendicular to the beam and  $\sim 4000$  in the pellicles exposed at  $20^\circ$ . The mean flux of antiprotons was  $4.3 \times 10^6$  per  $\text{cm}^2$  accumulated in 3.9 h.

### III. RESULTS AND DISCUSSION

From the number of stars observed and the measured flux of 2.9-GeV antiprotons, the star-production cross section was calculated to be  $880 \pm 100$  mb. This is to be compared with  $410 \pm 50$  mb for stars produced by 3.0-GeV incident protons.<sup>16</sup> The total reaction cross section of Ag with 430-MeV antiprotons is 1630 mb, of which 1500 mb are due to annihilation.<sup>17</sup> The total reaction cross section with 430-MeV protons is 1050 mb. Similar data are not available for higher antiproton energies.

More detailed comparative cross section data are presented in Table II. The  $\alpha$ -particle production cross section is almost three times as large when the incident particles are antiprotons. Even on a per star basis, about one-third more  $\alpha$ 's are emitted. The differences for emission of light fragments are not quite as large, but the trend is the same. In Fig. 1, the prong multiplicities of the  $\alpha$  particles and light fragments are compared for proton and antiproton irradiations.<sup>18</sup> Clearly, the latter

<sup>16</sup> S. Katcoff (unpublished).

<sup>17</sup> L. E. Agnew, O. Chamberlain, D. V. Keller, R. Mermod, E. H. Rogers, H. M. Steiner, and C. Wiegand, Phys. Rev. **108**, 1545 (1957).

<sup>18</sup> Prong multiplicities were obtained by considering also the steeper tracks and those that left the emulsion. For the  $\alpha$  particles, this procedure appears to be satisfactory since the number of  $\alpha$ 's per star computed from the prong multiplicities agrees within a few percent with the values given in Table II. For the light fragments, this procedure underestimates the number per star by about 30%. However, the comparisons of the prong multiplicities from the antiproton and the proton irradiations are entirely valid since the same procedure was used in both cases. The results given

produce larger stars; antiprotons deposit substantially more energy in complex nuclei than protons do. It is difficult to compare the relative excitation energies quantitatively because of the star-selection criteria. If we assume that the fraction of unobserved stars is the same in both cases, the  $\alpha$ -particle data indicate that about one-third larger mean excitation energies are produced by the antiproton irradiation. On the other hand, if we assume that the total reaction cross sections are roughly the same at 3.0 GeV as at 430 MeV, the  $\alpha$ -particle data suggest a mean excitation that is about 80% larger when the projectiles are antiprotons.

The cross section for production of hammer tracks (mostly  $\text{Li}^9$ ) is about sevenfold higher in the antiproton irradiation (Table II). For light fragments in general, it is only 2.6-fold higher. This observation suggests that neutron-rich products are more probable when targets are irradiated by the negatively charged antiproton rather than the positively charged proton. In effect, it is as though  $Z$  of the target were decreased by two units without changing its mass. This is equivalent to increasing the neutron to proton ratio  $N/Z$  from 1.26 to 1.37. It has already been shown<sup>19</sup> that such a change in  $N/Z$  increases the cross section of  $\text{Li}^9$  by a factor of two.

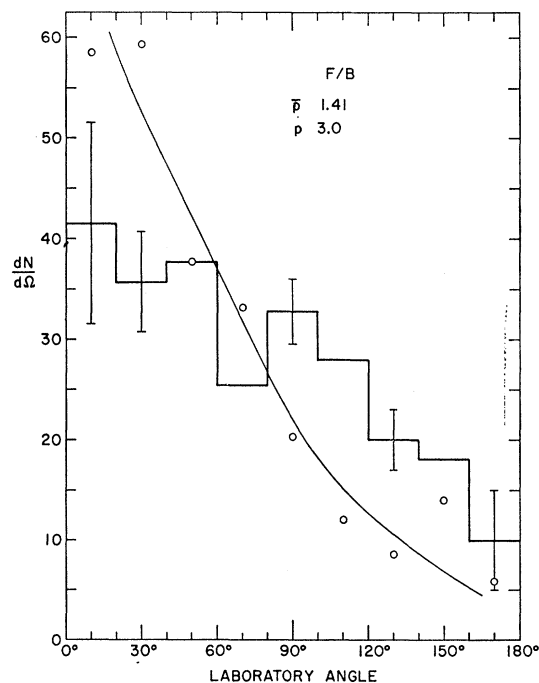


Fig. 3. Angular distribution of the nuclear recoils to the beam. Histogram—antiproton irradiation; curve with points—proton irradiation.

here for the 3.0-GeV proton bombardment (Table II and Fig. 1) differ slightly from those given previously (Ref. 11), because now the correction for small unobserved stars has been omitted.

<sup>19</sup> I. Dostrovsky, R. Davis, Jr., A. M. Poskanzer, and P. L. Reeder, Phys. Rev. **139**, B1513 (1965).

It should be noticed in Table II that the cross sections for production of type-III stars (characterized by two short very dense tracks) are about the same for both types of incident particles. On the other hand, type-II stars (light-fragment stars) are much more probable per incident antiproton than per incident proton. In addition, for the antiproton irradiation, type-III stars are deficient in  $\alpha$  prongs by about a factor of two in comparison with the other stars; for the proton irradiation the number of  $\alpha$  prongs per star is independent of star type. A similar effect is indicated for the light fragment prongs in type-III stars, but the statistics are very poor. These differences in behavior support the idea that stars of types II and III are produced by different mechanisms.<sup>14</sup>

Because of the somewhat higher number of emitted particles per star, one might expect some increase in the mean range of the recoil nuclei. This seems to be the case. For incident antiprotons, the mean range is  $4.5 \pm 0.1 \mu$ , compared to  $4.2 \pm 0.1 \mu$  for incident protons. Both recoil range distributions are shown in Fig. 2. The angular distribution of the recoils (Fig. 3) is not as forward-peaked for an antiproton irradiation. The forward-to-backward ratio is 1.4 rather than 3.0 (for proton irradiation). This is related to the fact that for a given momentum transfer from the projectile, more excitation energy is deposited in the target nuclei in the case of antiprotons. Consequently, a higher proportion of the recoil momentum results from particle evaporation, and this portion is more nearly isotropic. Furthermore, peripheral interactions which lead to high excitation are considerably more probable for antiproton bombardment.

The normalized spectra of the emitted  $\alpha$  particles are compared in Fig. 4. The spectrum which corresponds to the antiproton irradiation (histogram) is broader and it shows relatively more low-energy  $\alpha$ 's. Again, a higher nuclear temperature is indicated. The angular distribution of the  $\alpha$  particles with respect to the beam is shown in Fig. 5. Although there seems to be a peak near  $90^\circ$ ,

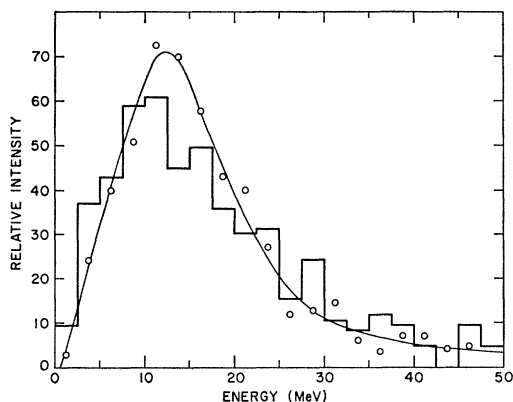


FIG. 4.  $\alpha$ -particle spectra. Histogram—antiproton irradiation; curve with points—proton irradiation.

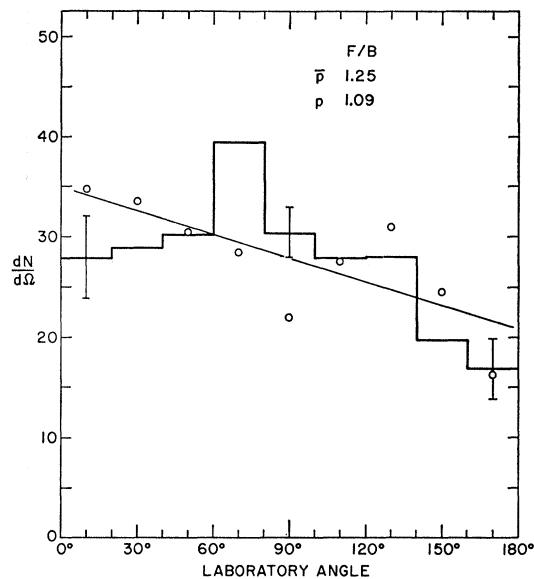


FIG. 5. Observed angular distribution of  $\alpha$ 's with respect to the beam. Histogram—antiproton irradiation; curve with points—proton irradiation.

the statistical errors make this uncertain. Table III shows that the forward-to-backward ratio (1.25) may be slightly larger than it is in 3.0-GeV proton irradiation (1.09). The corresponding difference for low energy  $\alpha$ 's ( $\leq 10$  MeV) is much greater:  $F/B=1.12$  for antiprotons and 0.59 for protons. As with proton irradiation,<sup>10,20</sup> these low-energy  $\alpha$  particles tend to be emitted in the backward direction relative to the motion of the recoil (Fig. 6).

The angular distributions of the light fragments for both proton and antiproton irradiations are shown in Fig. 7. Although the statistical errors are large, both distributions look similar and show what has been considered<sup>11</sup> to be a deficiency of emission in the more forward directions ( $< 60^\circ$  laboratory angle). This effect has been related to light fragment emission on a fast time scale and to a reduced probability for very energetic interactions near the forward surface of the nucleus.

#### IV. CONCLUSION

It has been shown that when antiprotons interact with complex nuclei very large amounts of energy may

TABLE III. Summary of forward/backward ratios.

Prong and reference direction	Antiprotons	Protons
Recoils to the beam	$1.41 \pm 0.13$	$3.0 \pm 0.4$
$\alpha$ 's ( $\leq 50$ MeV) to beam	$1.25 \pm 0.08$	$1.09 \pm 0.09$
$\alpha$ 's ( $\leq 10$ MeV) to beam	$1.12 \pm 0.12$	$0.59 \pm 0.09$
$\alpha$ 's ( $\leq 50$ MeV) to recoil	$0.57 \pm 0.05$	$0.53 \pm 0.05$
$\alpha$ 's ( $\leq 10$ MeV) to recoil	$0.37 \pm 0.05$	$0.28 \pm 0.05$
Light fragments to beam	$1.3 \pm 0.2$	$1.8 \pm 0.3$

<sup>20</sup> N. T. Porile, Phys. Rev. **135**, B371 (1964).

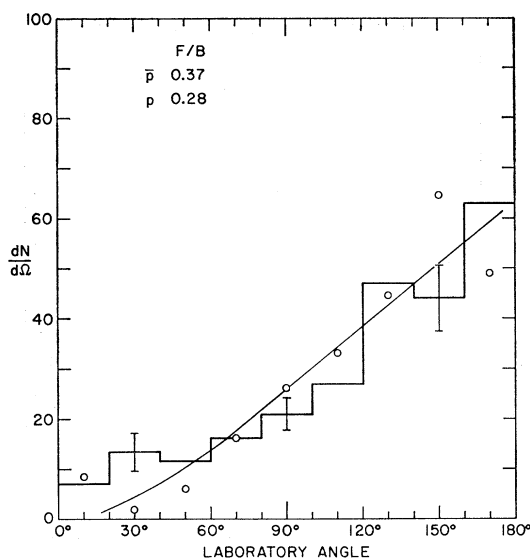


FIG. 6. Observed angular distribution of the low energy  $\alpha$ 's ( $\leq 10$  MeV) with respect to the recoil. Histogram—antiproton irradiation; curve with points—proton irradiation.

be deposited. The mean excitation energy at 2.9-GeV incident kinetic energy is substantially higher than for comparable proton irradiations.  $\alpha$ -particle and light-fragment emission are considerably more abundant. Therefore, the lighter residual nuclei, those farther displaced from the target, should have relatively higher cross sections, while those with masses close to the target should be relatively less abundant. Furthermore, the products may tend to be somewhat more neutron-rich.

The radiochemical studies of Bell *et al.*<sup>1</sup> failed to demonstrate these effects because of low beam in-

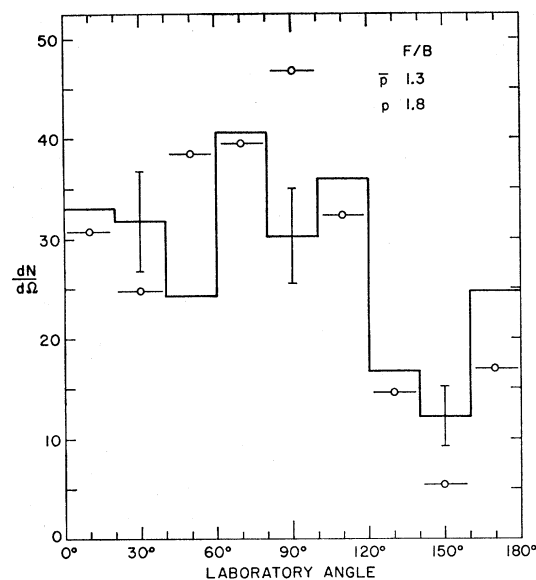


FIG. 7. Observed angular distribution of the light fragments with respect to the beam. Histogram—antiproton irradiation; horizontal bars with points—proton irradiation.

tensity and unfavorable targets and products. When more intense antiproton beams become available, the radiochemical experiments should give definitive results.

#### ACKNOWLEDGMENTS

It is a pleasure to thank Mrs. Doris Franck and Mrs. Dorothea Hodgdon for their careful and thorough-scanning of the emulsions and for assistance in processing the data. Special thanks are due to Hugh N. Brown and J. R. Sanford for assistance with the separated antiproton beam.